A New Method for Measuring Small Local Vibrations in the Heart Using Ultrasound

Hiroshi Kanai, *Member, IEEE*, Hiroaki Satoh, Kouichi Hirose, and Noriyoshi Chubachi, *Member, IEEE*

Abstract—**In order to diagnose ventricular dysfunction based on the acoustic characteristics of the heart muscle of the ventricle, it is necessary to detect vibration signals from various parts of the ventricular wall. This is, however, difficult using previously proposed ultrasonic diagnostic methods or systems. The reason is that the amplitude of the cardiac motion is large during one beat period which produces large fluctuations in the transit time required for ultrasonic waves to travel from the transducer to the heart and back. This paper proposes a new method for overcoming this problem and accurately measuring small vibrations of the ventricle wall using ultrasound. In this method, the demodulated ultrasound signal reflected at the heart wall is converted from analogue to digital (A/D) signal at a high sampling frequency; from the resultant digital signal, the velocity of the wall is accurately obtained over a wide dynamic range based on the Doppler effect. The proposed method is preliminarily applied to the detection of small vibrations on the aortic wall and the interventricular septum. The new method offers potential for research in acoustical diagnosis of heart and artery dysfunction.**

I. Introduction

THE need for a method to quantitatively measure heart sounds and heart wall vibrations during the cardiac cycle is becoming increasingly important [1], [2]. We have already proposed a new method for estimating the spectral transition of heart sounds between short-length signals of succeeding frames in low SNR cases [3]. By applying this method to the analysis of multiframe signals of the fourth heart sound obtained during a stress test, significant differences between the spectral transition patterns of 10 patients with myocardial infarction and 10 normal subjects were clearly detected. The significant characteristics of these transition patterns may be applied to acoustic diagnosis of heart diseases. On the other hand, several methods to estimate the acoustic transfer function of a heart have been also proposed [4], [5] by analyzing heart sounds detected by a microphone or an accelerometer. However, when measuring a heart sound from the chest wall of a patient, it is difficult to avoid the influence of the transfer characteristics of the chest. Thus, in reported experiments [3], [5], heart sounds were detected by an accelerometer placed in the esophagus. However, esophageal probe placement is not well tolerated in the unanesthetized patient. Moreover, it is difficult to detect local vibrations of small areas of various parts of the ventricle wall.

It is, therefore, desirable to transcutaneously detect such local vibrations with a probe placed on the chest wall using ultrasonic. Since continuous-wave ultrasonic Doppler motion detection was first demonstrated [6], numerous elaborate techniques [7]–[15] have been proposed for acoustic measurement of blood velocity in a subject at a certain fixed point based on the Doppler effect.

Vibrations of heart walls with small amplitude (about $\pm 100\,\mu$m, up to at least a few hundred Hertz) are superimposed on the *motion* with large amplitude (about ± 15 mm, several Hertz) due to heartbeat during one cardiac cycle. Thus, there are large fluctuations (about $\pm 10\,\mu$s) in the transit period of an ultrasonic wave traveling from a transducer to an object in the heart and back. Since the previously developed ultrasonic methods or systems obtain the velocity from the Doppler-shift detected at a predetermined return-time for each transmitted RF pulse using analogue circuits, it is difficult to obtain the small local vibrations of a wall on large motion due to the heartbeat.

Several methods have been developed to measure the diameter of the arterial walls by tracking small arterial wall motion with low frequency components for the blood flow detection [16], [17], for evaluation of elastic properties of the walls [18]–[20], for measurement of pressures [21], and for monitoring fetal breathing [22], [23].

Several methods have been proposed and applied to measure arterial wall *motion* having large amplitudes [23]–[30] in which the zero-crossing point of the echo signal from an arterial wall is tracked for each transmitted RF pulse using the phase-locked loop (PLL) technique. As pointed out in [2], however, with each of these devices it has proven to be experimentally difficult to lock onto and remain locked to the desired echo. As theoretically described in Section II-C of this paper, for the measurement of small vibrations on the heart motion, it is necessary to consider both phase shift of the returned RF pulse due to the instantaneous change of the object position and the Doppler-shift. In these method using the PLL circuit, the phase shift due to the Doppler-shift is neglected. Thus, it is difficult to accurately track the return time of each transmitted RF pulse by the PLL circuit. In these experimental systems, moreover, the detected signals are not vibrations but motions of the heart or artery wall. Thus, it is also difficult to measure small *vibrations* of the object in the frequency range up to a few hundred Hertz.

Manuscript received October 15, 1991; revised May 6, 1993. This work was supported in part by a Grant-in-Aid for Scientific Research (No. 04750392, 04555092, 05750389, 05555108) form the Ministry of Education, Science, and Culture of Japan and in part by TEPCO Research Foundation.

The authors are with the Department of Electrical Engineering, Tohoku University, Sendai 980, Japan.

IEEE Log Number 9213248.

To overcome the difficulties of tracking echo signals, an open-loop approach was employed in measuring small displacement such as vessel wall motion [20] and tissue deformation [31], and in measuring myocardial thickening of open chest dogs [2]. However, these methods cannot be applied to transcutaneous measurement of small *vibrations* of the myocardium with large amplitudes during the cardiac cycle in humans.

This paper proposes a new method for measuring small vibrations on various parts of the heart in the frequency range of up to a few hundred Hertz for the purpose of a acoustical diagnosis of dysfunction in the heart. As described in Section II-C, by considering both the phase shift of the returned pulse due to the instantaneous change of the object position and the Doppler shift, the equation for estimating the velocity of the object is newly derived. In order to realize this new method, the demodulated signal of the received signal is A/D converted at a high sampling frequency and the return time of each transmitted pulse is determined from the amplitude of the envelope signal of the received echo signal. From simulation experiments in Section V, the accuracy of the proposed method is evaluated. There are three boundary lines for the available region in the frequency-amplitude space and these are theoretically explained in Sections III and IV. Based on the proposed method, we have conceptualized a measurement system to detect vibration signals over a wide dynamic range. From experiments using a water tank which simulates the small vibrations of the heart wall superimposed on the motion with large amplitude due to heart beat, the accuracy of the proposed method is evaluated in Section VI. Finally in Section VII, as a preliminary experiment, the proposed method is applied to the detection of small vibrations on the aortic wall near the aortic valve and the interventricular septum wall in a human.

II. Principle

A. Definition of Signals and Doppler Effect

The transmitted RF pulse $V_{in}(t)$ with angular-frequency ω_0 in Fig. 1(a) is denoted by

$$V_{in}(t) = A_{in}\mathrm{Re}[\exp(j\omega_0 t)]\{u(t) - u(t - T_0)\} = A_{in}\frac{\exp(j\omega_0 t) + \exp(-j\omega_0 t)}{2}\{u(t) - u(t - T_0)\} \quad (1)$$

where $u(t)$, T_0, and A_{in} are the unit step function, the pulse width, and the pulse amplitude, respectively, and Re[·] shows the real part. Let us assume that the RF pulses $V_{in}(t)$ are transmitted at a time interval ΔT as shown in Fig. 1(a) and (b). Defining the acoustic velocity as c, the instantaneous distance $x(t)$ between an ultrasonic transducer and a moving object in a heart is denoted by $x(t) = c \cdot \tau_t$ where τ_t is the period required for one-way transmission from the object to the ultrasonic transducer. Let us assume that $\tau_t < (\Delta T/2)$.

In the received signal $V_{out}(t)$ of Fig. 1(a) and (b), the angular-frequency ω_0 is shifted by $\Delta\omega_t$ due to the Doppler effect, the magnitude of which is approximately obtained from

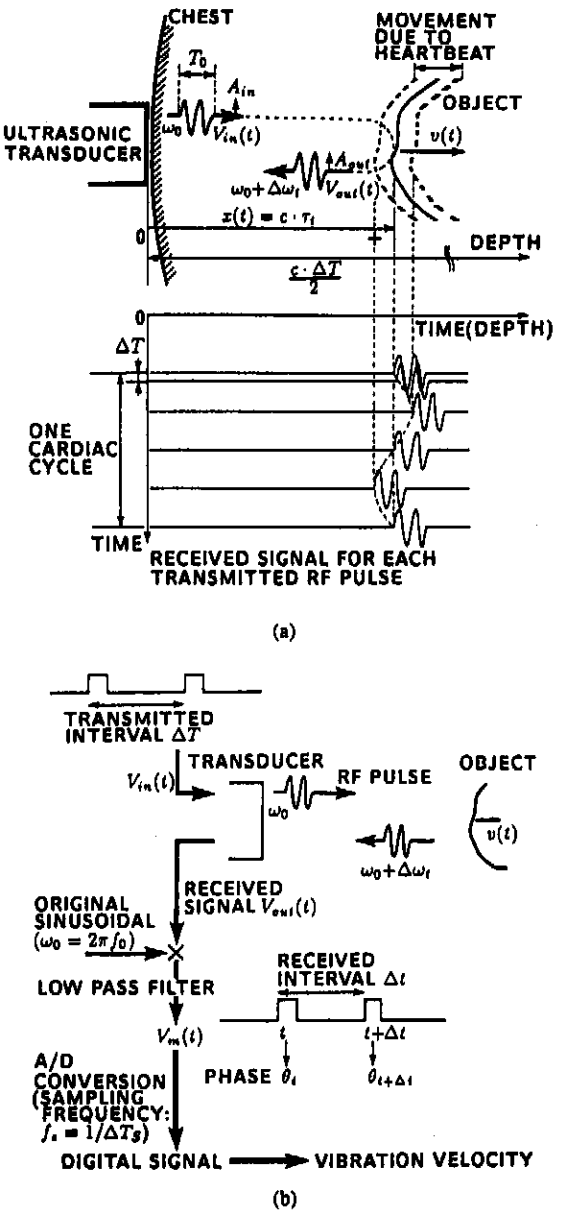

Fig. 1. (a) An illustration explaining the transmitted wave $V_{in}(t)$ from an ultrasonic transducer and its reflective wave $V_{out}(t)$ from an object. (b) Outline of the measurement procedure proposed in this paper.

the velocity magnitude $v(t)$ of the object by

$$\Delta\omega_t = \omega_0\frac{1 - v(t)\cos\theta/c}{1 + v(t)\cos\theta/c} - \omega_0 \simeq -2\omega_0\frac{v(t)}{c}\cos\theta, \quad \text{for } \frac{v(t)}{c} \ll 1$$

where θ denotes the angle between the sound beam and the velocity vector. The vector velocity $\vec{v}(t)$ corresponds to the superposed components of the small vibration and the motion due to heartbeat. Since the angle θ is determined by the B-mode image in the standard system, we assume that $\vec{v}(t)$ is parallel to the transmission direction of the ultrasonic beam. Thus, the angular-frequency shift $\Delta\omega_t$ is denoted by

$$\Delta\omega_t \simeq -2\omega_0\frac{v(t)}{c}. \quad (2)$$

The received signal $V_{out}(t)$ in Fig. 1 is described as

$$V_{out}(t) = A_{out}\mathrm{Re}\left[\exp\left\{j\left(\omega_0 t + \int_{-\infty}^{t}\Delta\omega_{t'}dt' - (2\omega_0 + \Delta\omega_t)\tau_t + \Omega\right)\right\}\right] \times \{u(t-2\tau_t) - u(t-T_0-2\tau_t)\} \quad (3)$$

where A_{out} denotes the amplitude of the received signal. The term $\exp\{j(\omega_0 t + \int_{-\infty}^{t}\Delta\omega_{t'}dt')\}$ denotes the sinusoidal wave having an instantaneous angular frequency of $\omega_0 + \Delta\omega_t$. The two components $\exp\{-j\omega_0\tau_t\}$ and $\exp\{-j(\omega_0+\Delta\omega_t)\tau_t\}$ in the term $\exp\{-j(2\omega_0+\Delta\omega_t)\tau_t\}$ denote the phase shifts due to the propagation of the ultrasonic wave with ω_0 from the transducer to the object and the propagation of the reflective wave with $\omega_0 + \Delta\omega_t$ from the object to the transducer, respectively. The term $\exp\{j\Omega\}$ describes the phase shift due to the reflection of an ultrasonic wave at the surface of the object. This term is approximately considered as a constant value during one cardiac cycle. By multiplying $V_{out}(t)$ by the complex signal $\exp\{j\omega_0 t\}$ of the original sinusoidal and passing the result through a low-pass filter as shown in Fig. 1(b), the low-frequency component $V_m(t)$ of the demodulated complex signal is obtained as follows:

$$V_m(t) = \frac{1}{2}A_{out}\exp\left\{-j\left(\int_{-\infty}^{t}\Delta\omega_{t'}dt' - (2\omega_0+\Delta\omega_t)\tau_t + \Omega\right)\right\} \times \{u(t-2\tau_t) - u(t-T_0-2\tau_t)\}. \quad (4)$$

If $V_m(t)$ is A/D converted at a frequency ($= 1/\Delta T_S$) which almost corresponds to the ultrasonic frequency $f_0 = \omega_0/2\pi$, the received pulse position is detected with high accuracy by analyzing the resultant digital signal. From (4), the phase θ_t of the received pulse is described by

$$\theta_t = -\int_{-\infty}^{t}\Delta\omega_{t'}dt' + (2\omega_0+\Delta\omega_t)\tau_t - \Omega. \quad (5)$$

In the Doppler detection using continuous ultrasonic waves, the velocity $v(t)$ and the distance $x(t)$ between the transducer and the object are considered to be a constant value. By substituting $\Delta\omega_t$ and τ_t in (4) by constant values $\Delta\omega_0 = -2\omega_0 v_0/c$ and τ_0, respectively, the low-frequency component of the demodulated signal $V_m(t)$ is described by the sinusoidal wave as follows:

$$V_m(t) = A_{out}\exp\{-j(\Delta\omega_0 t + \Omega_1)\}$$

where

$$\Omega_1 = -(2\omega_0 + \Delta\omega_0)\tau_0 + \Omega.$$

By estimating the Doppler shift $\Delta\omega_0$ from $V_m(t)$, the velocity v_0 is determined. Thus, in the Doppler detection with continuous waves, only the first term in the right-hand side of (5) is evaluated.

B. Standard Pulse Doppler Method

When the RF pulses of (1) are transmitted at a time interval ΔT, let us denote the time interval between a pulse received at time t and the succeedingly received pulse by Δt as shown in Fig. 1(b), which is almost equal to ΔT but which is a time-dependent parameter because the object is moving with large amplitude. Let us define the velocity of the object, $v(t+\Delta t/2)$, at a middle time, $t + \Delta t/2$, of the period Δt between one received pulse and the succeeding pulse by

$$v\left(t+\frac{\Delta t}{2}\right) \equiv \frac{x(t+\Delta t) - x(t)}{\Delta t}$$

where the term $x(t+\Delta t) - x(t)$ in the right-hand side is denoted by

$$x(t+\Delta t) - x(t) = c\cdot(\tau_{t+\Delta t} - \tau_t)$$

which corresponds to the distance that the object moves for the time interval Δt. Thus, the velocity $v(t+\Delta t/2)$ is denoted by

$$v\left(t+\frac{\Delta t}{2}\right) = c\cdot\frac{\tau_{t+\Delta t} - \tau_t}{\Delta t}. \quad (6)$$

In the standard pulse Doppler system, the period τ_t is assumed to be a constant value τ_0, that is, $\Delta t = \Delta T$. Thus, only the first term $\int_{-\infty}^{t}\Delta\omega_{t'}dt'$ in (5) is considered as

$$\theta_t = -\int_{-\infty}^{t}\Delta\omega_{t'}dt' - \Omega_1.$$

By differentiating both sides by t,

$$\frac{d\theta_t}{dt} = -\Delta\omega_t. \quad (7)$$

By approximating $(d\theta_t/dt)$ by $(\theta_{t+\Delta T} - \theta_t)/\Delta T$ and substituting $\Delta\omega_t$ of (2) into $\Delta\omega_t$ in the right-hand side, the velocity is obtained by

$$v\left(t+\frac{\Delta T}{2}\right) = \frac{c}{2\omega_0}\cdot\frac{\theta_{t+\Delta T} - \theta_t}{\Delta T}. \quad (8)$$

This standard estimation procedure depends only on the detection of the Doppler-shift angular-frequency $\Delta\omega_t$ of the first term in (5).

C. Proposed Method

In the measurement of small vibrations on the heart motion, however, phase shift due to the instantaneous position of the object denoted by the second term, $2\omega_0\tau_t$, in (5) cannot be neglected, as described below. Using (2) and the relation $x(t) = \int_{-\infty}^{t}v(t')dt'$, the phase θ_t of (5) is re-expressed as follows:

$$\theta_t = 2\omega_0\frac{x(t)}{c} + (2\omega_0+\Delta\omega_t)\tau_t - \Omega = 4\omega_0\tau_t + \Delta\omega_t\tau_t - \Omega. \quad (9)$$

Since $\Delta\omega_t \ll \omega_0$, $\Delta\omega_t$ can be neglected in (9). As a result, the phase θ_t of (9) is approximated by the product between the ultrasonic angular-frequency ω_0 and the transmission time τ_t as

$$\theta_t \simeq 4\omega_0\tau_t - \Omega. \quad (9')$$

This equation (9′) is derived by considering both the phase shift due to the instantaneous change of the object position in the second term of (5) and the Doppler-shift in the first term of (5). Many methods have been proposed for detecting aortic wall motion by tracking the zero-crossing point of the returned RF pulse using the phase-locked loop (PLL) circuit [24]–[30] as described previously. These methods consider only the phase shift due to the instantaneous change of the object position in the second term of (5). That is, the phase shift due to the Doppler-shift in the first term of (5) is neglected. However, as theoretically shown in (9), the phase shift, $(2\omega_0+\Delta\omega_t)\tau_t \simeq 2\omega_0\tau_t$, which is due to the change of the object position is almost equal to the term $-\int_{-\infty}^{t}\Delta\omega_{t'}dt' = 2\omega_0\tau_t$, due to the Doppler-shift. That is, the zero-crossing point moves left or right in the time domain according to both effects. Thus, the previous PLL-based methods cannot track aortic wall motion.

Based on the relation shown in (9′), we propose an alternative new method to estimate the velocity $v(t)$ of an object moving with a large amplitude as described below. The phase difference $\theta_{t+\Delta t} - \theta_t$ between the demodulated signals of $V_{\text{out}}(t)$ and $V_{\text{out}}(t+\Delta t)$ is obtained by

$$\theta_{t+\Delta t} - \theta_t = 4\omega_0(\tau_{t+\Delta t} - \tau_t).$$

Using (6), the velocity $v(t)$ of the object is estimated as follows:

$$\hat{v}\left(t+\frac{\Delta t}{2}\right) = c\cdot\frac{\theta_{t+\Delta t}-\theta_t}{4\omega_0\Delta t}. \qquad (10)$$

Therefore, the vibration velocity $v(t)$ on a large amplitude motion is estimated from the phase change $\theta_{t+\Delta t}-\theta_t$ and the time interval Δt between the received pulses.

Since it is necessary for the proposed method in (10) to accurately track and detect the wall position, the demodulated signal $V_m(t)$ in (4) is A/D converted at a high sampling frequency as shown in Fig. 1(b). From the resultant digital complex signal $V_m(t)$, the position of each object is tracked by detecting the point which has the maximum in the amplitude signal $|V_m(t)|$ of $V_m(t)$ in a predetermined range of depth from the chest wall. The period, $2\times\tau_t$, required by an ultrasonic wave to travel from the ultrasonic transducer to the object and back is obtained for each transmitted pulse. The interval Δt of the received pulses is calculated from the values of τ_t and the transmitted interval ΔT of the RF pulses. The phase shift $\theta_{t+\Delta t}-\theta_t$ generated during the interval Δt is also obtained from $V_m(t)$ and $V_m(t+\Delta t)$.

The resultant velocity estimate $\hat{v}(t)$ is sampled at unequal intervals of Δt, which varies around the time interval ΔT of the transmitted pulses. In the experiments reported here, however, the vibration signal to be detected has only frequency components less than several hundred Hertz and the fluctuation of $\{\Delta t\}$ is within a few microseconds. Thus, the effect due to unequal interval sampling can be neglected for the vibration signal estimated in this paper.

III. Significance in Identifying the Periods Required for Transmission

Using a simple example, we show why it is significant to accurately identify the phase value θ_t and the time interval Δt from the digital signal which is A/D converted with high sampling frequency $(=1/\Delta T_S)$. For this purpose, let us define the displacement function $x(t)$ of an object by

$$x(t) = a_{x_0}\sin(2\pi f_{x_0}t) \qquad (11)$$

where a_{x_0} and f_{x_0} are the peak vibration amplitude and the vibration frequency, respectively. Then, the velocity function $v(t)$ of the object is obtained by

$$v(t) = \frac{dx(t)}{dt} = 2\pi a_{x_0}f_{x_0}\cos(2\pi f_{x_0}t). \qquad (12)$$

First, let us evaluate the maximum value $\Delta\theta_{\max}$ of $|\theta_{t+\Delta T_S}-\theta_t|$ due to the first term $4\omega_0\tau_t$ in the right-hand side of (9) as follows:

$$\begin{aligned}\Delta\theta_{\max} &= |\theta_{t+\Delta T_S}-\theta_t|_{\max}\\ &= |4\omega_0\cdot\tau_{t+\Delta T_S}-4\omega_0\cdot\tau_t|_{\max}.\end{aligned}$$

Using the relation $\tau_t = x(t)/c$ and assuming that the frequency f_{x_0} of (11) is sufficiently less than the sampling frequency $(=1/\Delta T_S)$,

$$\begin{aligned}\Delta\theta_{\max} &\simeq \frac{4\omega_0}{c}\left[\frac{d}{dt}x(t)\right]_{\max}\times\Delta T_S\\ &= \frac{8\pi\omega_0 a_{x_0}f_{x_0}\Delta T_S}{c}.\end{aligned} \qquad (13)$$

Next, let us evaluate the maximum value $\Delta\theta'_{\max}$ of the phase difference $|\theta_{t+\Delta T_S}-\theta_t|$ due to the second term $\Delta\omega_t\tau_t$ in the right-hand side of (9) as follows:

$$\begin{aligned}\Delta\theta'_{\max} &= |\theta_{t+\Delta T_S}-\theta_t|_{\max}\\ &= |\Delta\omega_{t+\Delta T_S}\cdot\tau_{t+\Delta T_S}-\Delta\omega_t\cdot\tau_t|_{\max}.\end{aligned}$$

Using (2) and the relation $\tau_t = x(t)/c$,

$$\begin{aligned}\Delta\theta'_{\max} &\simeq \frac{2\omega_0}{c^2}\left[\frac{d}{dt}(v(t)x(t))\right]_{\max}\times\Delta T_S\\ &= \frac{2\omega_0}{c^2}2\pi a_{x_0}^2 f_{x_0}\times\frac{1}{2}\left[\frac{d}{dt}\sin(4\pi f_{x_0}t)\right]_{\max}\times\Delta T_S\\ &= \frac{8\pi^2\omega_0 a_{x_0}^2 f_{x_0}^2\Delta T_S}{c^2}.\end{aligned} \qquad (14)$$

Since the ratio of $\Delta\theta_{\max}$ of (13) to $\Delta\theta'_{\max}$ of (14) is equal to $c/(\pi a_{x_0}f_{x_0})$, the approximation of (9′) holds for the cases where $\pi a_{x_0}f_{x_0} \ll c$.

Let us assume that $c = 1500$ m/s, $f_0 = 3.5$ MHz, and $\Delta T = 500\,\mu$s. For the cases where $f_{x_0} = 1.5$ Hz and $a_{x_0} = \pm 10$ mm and where $f_{x_0} = 100$ Hz and $a_{x_0} = \pm 150\,\mu$m, the maximum value $v_{\max}$ of the vibration velocity $v(t)$ of (12) is obtained by

$$v_{\max} = 2\pi a_{x_0}f_{x_0} = 0.0942\,[\text{m/s}] \ll 2c.$$

The maximum value $\Delta\theta_{\max}$ of (13) is obtained as

$$\Delta\theta_{\max} = 5.53\times10^3\times\Delta T_S[\text{rad}] = 0.317\times10^6\Delta T_S[\text{deg}].$$

For each case of $\Delta T_S = 1\,\mu s$, $\Delta T_S = 10\,\mu s$, and $\Delta T_S = 100\,\mu s$, the value $\Delta\theta_{max}$ is, respectively, obtained as 0.317 [deg], 3.17 [deg], and 31.7 [deg]. The evaluation of these values $\Delta\theta_{max}$ shows that there are large fluctuations in phase of the demodulated received pulse if the signal is A/D converted at a low-sampling frequency.

Using the maximum phase detection error $\Delta\theta_{max}$ and the maximum error $[\Delta t_e]_{max}$ in the detection of the time interval Δt, let us evaluate the maximum error Δv_{max} in the velocity estimated by (10) for the worst case as follows:

$$\Delta v_{max} = \frac{c}{4\omega_0} \cdot \frac{2 \times \Delta\theta_{max}}{\Delta T \pm [\Delta t_e]_{max}}.$$

Using $\Delta\theta_{max}$ of (13) and setting $\pm[\Delta t_e]_{max}$ as $-2 \times \Delta T_S$,

$$\Delta v_{max} = 2\pi a_{x_0} f_{x_0} \cdot \frac{2 \times \Delta T_S}{\Delta T - 2 \times \Delta T_S}. \tag{15}$$

For each case of $\Delta T_S = 1\,\mu s$, $\Delta T_S = 10\,\mu s$, and $\Delta T_S = 100\,\mu s$, the maximum estimation error Δv_{max} is, respectively, obtained as 0.000379 [m/s], 0.00393 [m/s], and 0.0628 [m/s]. Thus, in order to accurately detect the local vibration with small amplitude on a heart wall, it is necessary to set the sampling frequency as at least more than 100 kHz.

It is, therefore, important to identify the phase value θ_t and the time interval Δt, both of which are required for calculating (10), from the digital signal obtained with a high-sampling frequency.

IV. Limitation of the Proposed Method

Based on the sampling theorem, the absolute magnitude of the phase difference is required to be less than π. From (10), this condition determines the upper bound of the velocity estimates as follows:

$$|\hat{v}_{max}| < \left| \frac{c\pi}{4\omega_0 \Delta T} \right|. \tag{16a}$$

On the other hand, the lower bound of the velocity estimate is approximately obtained from (15) as

$$2\pi a_{x_0} f_{x_0} \frac{2\Delta T_S}{\Delta T - 2\Delta T_S} < |\hat{v}_{min}|. \tag{16b}$$

When $\Delta T = 500\,\mu s$, $f_0 = 3.5$ MHz, $c = 1500$ m/s, $\Delta T_S = 1\,\mu s$, and $a_{x_0} f_{x_0} = 0.015$ m·Hz, the maximum value $\hat{v}_{max}$ and the minimum value $\hat{v}_{min}$ of the velocity estimates are equal to 0.107 [m/s] and 0.000379 [m/s], respectively. Since the pulse repetition frequency $1/\Delta T$ is assumed to be 2 kHz, the effective frequency range of the estimated velocity signal $\hat{v}(t)$ is limited by 1 kHz ($= 1/2\Delta T$). The available region determined by these three values become broader by increasing the pulse repetition frequency.

V. Accuracy Evaluation by Simulation Experiments

In order to evaluate the accuracy in the vibration velocity $\hat{v}(t)$ of (10) estimated by the proposed method, the following simulation experiments were performed. The estimation error is evaluated by the following normalized squared difference

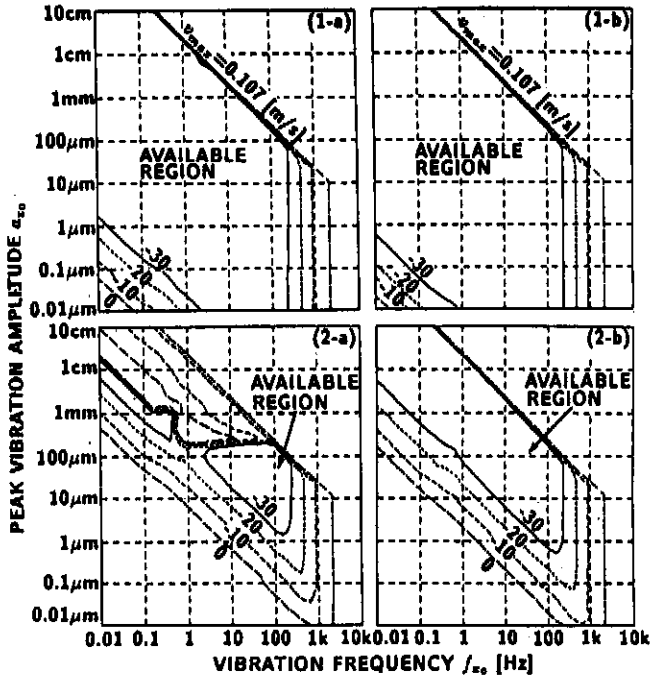

Fig. 2. The normalized squared error $\rho(a_{x_0}, f_{x_0})$ [dB] in the velocity $\hat{v}(t)$ estimated by the proposed method. (1) for $V_m(t)$ generated in computer with 32 b floating-point arithmetic. (2) for $V_m(t)$ generated in computer with 12 b integer arithmetic. (a) for $V_m(t)$ generated at a sampling rate of 10 μs. (b) for $V_m(t)$ generated at a sampling rate of 1 μs.

$\rho(a_{x_0}, f_{x_0})$ between the actual vibration velocity $v(t)$ and the estimated vibration velocity $\hat{v}(t)$ of (10) as

$$\rho(a_{x_0}, f_{x_0}) = \frac{\sum_t |\hat{v}(t) - v(t)|^2}{\sum_t |v(t)|^2} \tag{17}$$

which is normalized by the power of the actual vibration velocity $v(t)$. The normalized squared error $\rho(a_{x_0}, f_{x_0})$ is calculated for various values of the peak vibration amplitude a_{x_0} and the frequency f_{x_0} of (11) as shown in Fig. 2.

Fig. 2(1-a) and 2(1-b) show the results obtained from the low frequency component of the demodulated signal $V_m(t)$ generated in a computer using floating-point arithmetic (32 b accuracy). Fig. 2(2-a) and 2(2-b) show the results from $V_m(t)$ generated in a computer using integer arithmetic (12 b accuracy), which corresponds to the case where the real and imaginary parts of the complex signal $V_m(t)$ are A/D converted with a two-channel 12 b A/D converter. The results in Fig. 2(1-a) and 2(2-a) and those in Fig. 2(1-b) and 2(2-b) are, respectively, obtained from the signals $V_m(t)$ which are generated at sampling intervals ΔT_S of 10 μs and 1 μs. The values of the parameters c, f_0, and ΔT are set as 1500 m/s, 3.5 MHz, and 500 μs, respectively.

Available region is defined by the condition where the squared normalized error $\rho(a_{x_0}, f_{x_0})$ is less than -30 dB as shown in these figures. Each available region is limited on the right side by the pulse repetition frequency $1/\Delta T$. The upper right side of each available region is limited by the maximum value $|\hat{v}_{max}|$ of (16a), which also depends on the time interval ΔT. The lower-left side of each available region has close relationship with the minimum value $\hat{v}_{min}$ of (16b), though the value is obtained for the worst case

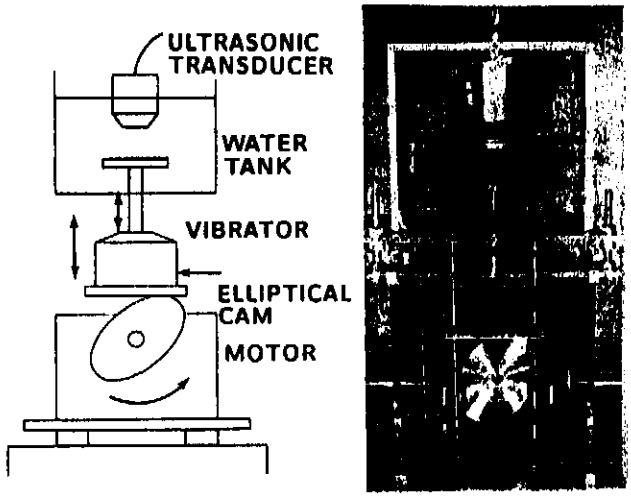

Fig. 3. A experimental system which simulates the vibration on the ventricle wall with heartbeat of large amplitude using a vibrator and a motor with an elliptical cam. The motor with the elliptical cam generates motion having a large amplitude of ±10 mm and a frequency of 1 Hz which corresponds to a heartbeat. The vibrator imposes a small amplitude vibration of up to about 100 Hz on this signal

without considering accuracy of the arithmetic. By increasing the repetition frequency of RF pulses, the available region becomes broader.

By comparing the results in Fig. 2(2-a) and 2(2-b) with those in Fig. 2(1-a) and (1-b), it is found that the available region is determined by the sampling interval ΔT_S and the sampling accuracy. The reason is that the measurement accuracy of the phase obtained from the signal $V_m(t)$ depends highly on these two parameters.

By increasing the sampling frequency $1/\Delta T_S$ of the signal $V_m(t)$ to 1 MHz as shown in Fig. 2(2-b), almost all of the region necessary for measurement of heart-wall vibrations is successfully covered by the proposed method.

VI. Experimental Results Using Water Tank

To confirm the principle of the proposed method, a small vibration signal $v(t)$ of a rubber plate in a water tank is estimated from the signal received by an ultrasonic transducer as shown in Fig. 3. The values of the parameters f_0, T_0, and ΔT are set at 3.5 MHz, 2 μs, and 250 μs, respectively. A motion with large amplitude (±10 mm, 1 Hz), which corresponds to heartbeat, is generated by the rotation of an elliptical cam. A vibration with small amplitude, which corresponds to the vibration on the wall of a ventricle, is generated by a vibrator on the elliptical cam. The received output signal of the ultrasonic transducer is amplified and demodulated. Then, the resultant real and imaginary signals are simultaneously A/D converted with a 12 b A/D converter at a sampling rate of 1 MHz. The length of each signal is about 512×10^3 points (= 0.512 s). The input voltage signal of the vibrator and the output signal of a laser displacement meter (Anritsu KL135A, Minami-azabu 5-10-27, Tokyo, Japan) are also A/D converted simultaneously.

Figs. 4 and 5 show the results of these estimations. We generated two types of small vibration; Fig. 4 corresponds to a sinusoidal wave of $f_{x_0} = 80$ Hz ($a_{x_0} = \pm 80\,\mu$m) and Fig. 5 corresponds to white noise in the frequency band ranging from 30 to 100 Hz ($a_{x_0} = \pm 80\,\mu$m). The vibrator generates displacement of the plate which corresponds to the input voltage signal. Thus, after differentiating the input voltage signals, Figs. 4(d) and 5(e) show the resultant signals $V_{\text{input}}(t)$, which correspond to a vibration velocity with small amplitude of the rubber plate. Figs. 4(a) and 5(a) show the period, $2 \times \tau_t$, required for the ultrasonic wave to travel from the ultrasonic transducer to the rubber plate and back. This period is determined without phase information from the timing when the amplitude of each received pulse has a local maximum. These lines correspond to those detected by standard ultrasonic diagnosis systems.

Fig. 4(b) shows the vibration velocity signal $\hat{v}(t)$ estimated by the proposed method and its spectrum. The resultant power spectrum has two main peaks which correspond to the small vibration due to the vibrator and the motion due to the rotating elliptical cam. The amplitude of the signal $\hat{v}(t)$ in Fig. 4(b-1) almost coincides with that of the signals $v_{\text{laser}}(t)$ obtained by differentiating the output signal of the laser displacement meter in Fig. 4(c). The output signal of the laser displacement meter is passed through a high-pass filter (cutoff frequency $f_c = 60$ Hz) before A/D conversion to remove the components due to motion of the elliptical cam with large amplitude.

Fig. 5(b) shows the vibration velocity signal $\hat{v}(t)$ estimated by the proposed method and its power spectrum. After removing the components due to motion with large amplitude by a digital high-pass filter (cut-off frequency $f_c = 30$ Hz), the waveform of the resultant signal shown in Fig. 5(c) almost coincides with both waveforms of the velocity signal $v_{\text{laser}}(t)$ of Fig. 5(d) obtained from the laser displacement meter and of the differentiated original signal $V_{\text{input}}(t)$ in Fig. 5(e).

For comfirming the correlation at each frequency between the estimated signal $\hat{v}(t)$ and the velocity signal $v_{\text{laser}}(t)$ obtained from the laser displacement meter, the following coherence function $\gamma^2(f)$ is calculated.

$$\gamma^2(f) = \frac{|E[\hat{V}(f)^* V_{\text{laser}}(f)]|^2}{E[|\hat{V}(f)|^2]E[|V_{\text{laser}}(f)|^2]} \tag{18}$$

where $\hat{V}(f)$ and $V_{\text{laser}}(f)$ are the spectra of $\hat{v}(t)$ and $v_{\text{laser}}(t)$, respectively. The term $E[\cdot]$ and * denote the average operation and the complex conjugate, respectively. The number of the averaging is equal to 16 times in this experiment. Fig. 5(f) shows the coherence function $\gamma^2(f)$ between $\hat{v}(t)$ and $v_{\text{laser}}(t)$. From these experimental results, the small vibration on the large motion is successfully detected in a frequency range up to greater than 100 Hz.

VII. Preliminary Experiments for Detecting Vibrations on the Aortic Wall and the Heart Wall

Figure 6 shows preliminary results obtained by applying the proposed method to the detection of a vibration signal on the back wall of the aorta near the aortic valve in a young man. The values of the parameters f_0, T_0, and ΔT are set at 3.5 MHz, 2 μs, and 250 μs, respectively.

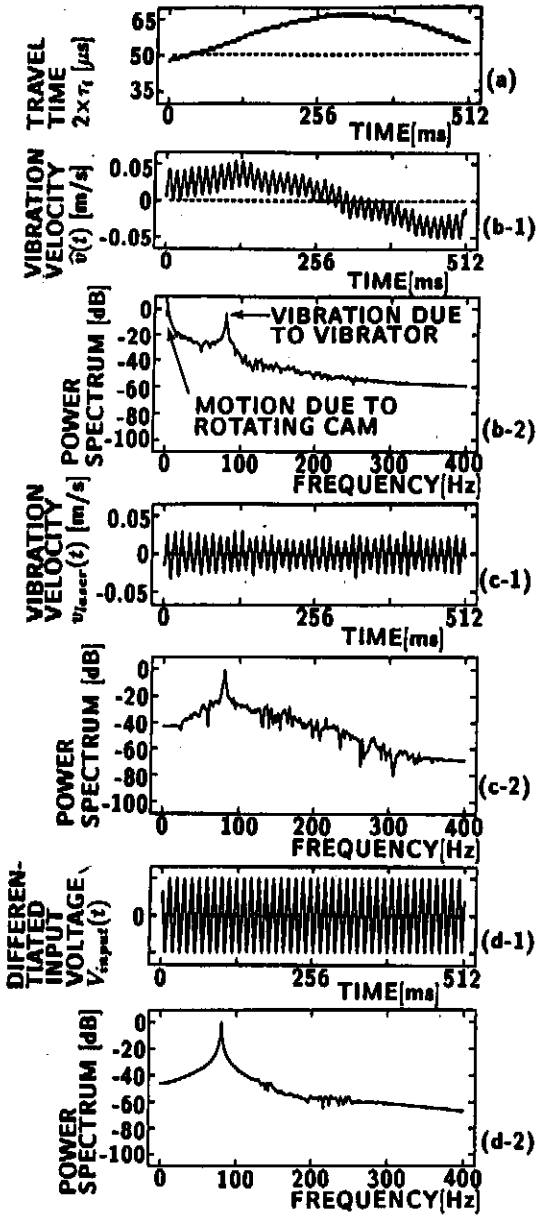

Fig. 4. Estimation results using the experimental system in Fig. 3. The vibrator generates an 80 Hz sinusoidal wave with an amplitude of about $\pm 80\,\mu$m. (a) The transit period, $2 \times \tau_t$, required by the ultrasonic wave to travel from the ultrasonic transducer to the rubber plate and back in the water tank. (b) The vibration velocity signal $\hat{v}(t)$ estimated by the proposed method from the output signal of the ultrasonic transducer and its power spectrum. (c) The velocity signal $v_{laser}(t)$ obtained by differentiating the output signal of a laser displacement meter and its power spectrum. (d) Differentiated input voltage signal $V_{input}(t)$ of the vibrator and its power spectrum.

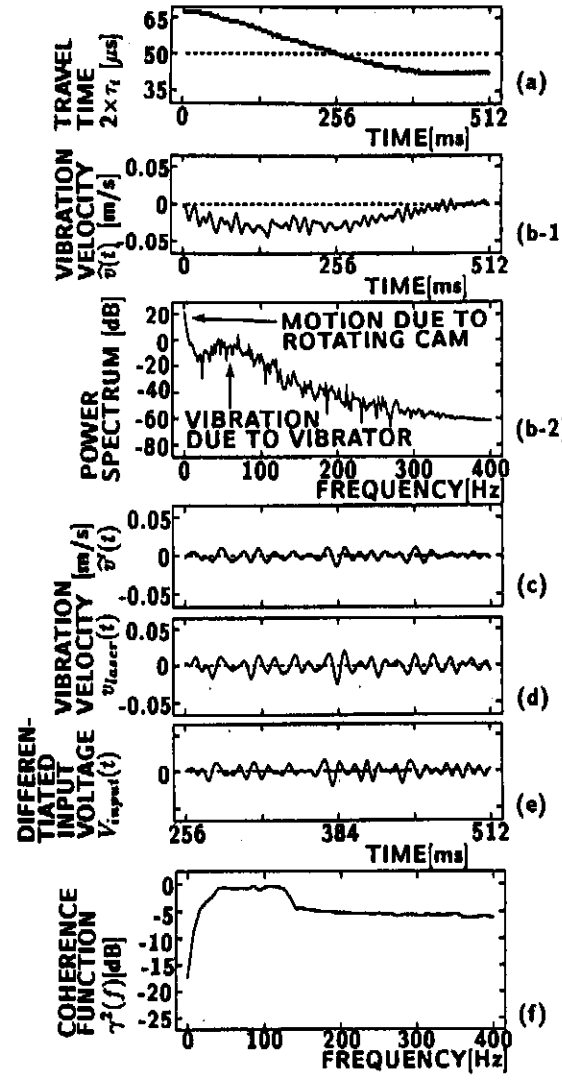

Fig. 5. Estimation results using the experimental system in Fig. 3. The vibrator generates a vibration of white noise (30–100 Hz) with an amplitude of $\pm 80\,\mu$m. (a) The transit period, $2 \times \tau_t$, required by the ultrasonic wave to travel from the ultrasonic transducer to the rubber plate and back. (b) The vibration velocity signal $\hat{v}(t)$ estimated by the proposed method from the output signal of the ultrasonic transducer and its power spectrum. (c) After applying a high-pass filter (cut-off frequency, $f_c = 30$ Hz) to the waveform in Fig. 5(b) to remove the low frequency components with large amplitude caused by the rotation of the elliptical cam, the latter half of the velocity waveform $\hat{v}'(t)$ of Fig. (b) is magnified. (d) The vibration signal $v_{laser}(t)$ obtained by differentiating the output signal of the laser displacement meter. The output signal is passed through a high-pass filter ($f_c = 30$ Hz) to remove the low frequency components with large amplitude before A/D conversion. (e) Differentiated input voltage signal $V_{input}(t)$ of the vibrator. (f) Coherence function $\gamma^2(f)$ between the vibration velocity signal $v_{laser}(t)$ and the detected vibration signal $\hat{v}(t)$.

Fig. 6(1) shows the electrocardiogram (ECG), which is simultaneously A/D converted by the A/D converter described above. Fig. 6(2) shows the period, $2 \times \tau_t$, required by an ultrasonic wave to travel from the ultrasonic transducer to the object and back. At the beginning of the ejection time (ET), the back wall is moving away from the ultrasonic transducer. Fig. 6(3) shows the amplitude of the received pulse.

Fig. 6(4) shows the vibration velocity of the aortic wall, which is obtained after applying the digital low-pass filter (cutoff frequency $f_c = 300$ Hz) to the vibration velocity estimated by the proposed method. Fig. 6(2) corresponds to the large motion of the aortic wall as shown in the M-mode image obtained by the standard ultrasonic diagnosis system. The resultant signal in Fig. 6(4) is, on the other hand, obtained from the phase of the received signal, and the vibration signal shows both components, namely, the large motion and the small vibration.

Especially at the beginning and the end of the ejection time (ET), vibrations with high frequency components are

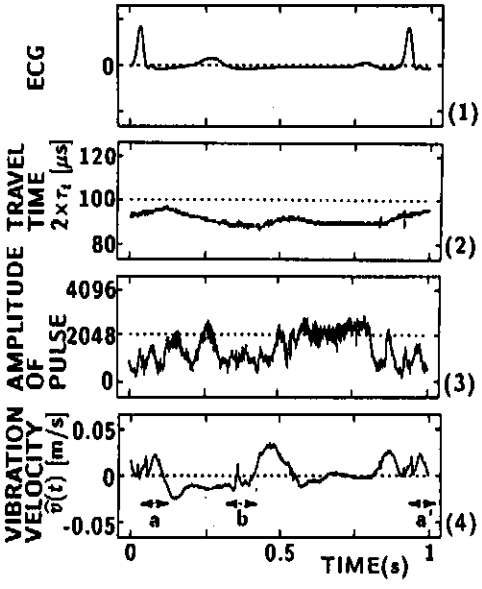

Fig. 6. Estimation results of the small vibration on the aortic wall near the aortic valve in a young man. (1) The electrocardiogram (ECG). (2) The transit period, $2 \times \tau_i$, required by the ultrasonic wave to travel from the ultrasonic transducer to the one side of the aortic wall and back. (3) The amplitude of the received pulses. The maximum scale of the amplitude is 4096, which corresponds to 12-bit accuracy in the A/D conversion. (4) The estimate of the vibration velocity on the aortic wall.

detected as shown in Fig. 6(4). The vibration in period (b) is due to the closing of the aortic valve. The two vibrations in periods (a) and (a′) in Fig. 6(4) are due to the opening of the aortic valve. The signals in these periods, (a) and (a′), almost coincide with each other. Thus, from these preliminary experiments for detecting the vibration velocity of the aortic wall near the aortic valve, reproducibility of the measurement was confirmed.

Fig. 7 shows the results of the experiment for the detection of small vibrations on the wall of the interventricular septum in the same young man as in the experiments in Fig. 6. Fig. 7(1) and (2), respectively, show the ECG and the detected vibration signal on the wall of the interventricular septum by the proposed method. The refection position of each RF ultrasonic wave in the interventricular septum is determined from the local maximum amplitude of the received signal. The values of the parameters f_0, T_0, and ΔT are the same as those of the experiments in Fig. 6. The signals detected in periods (a) and (a′) at the beginning of the ejection time almost coincide with each other. There are several pulses in one cardiac cycle. The physical meaning of the pulses obtained in Fig. 7(2) is currently under investigation.

VIII. Concluding Remarks

This paper proposes a new method for measurement of small vibrations on a large motion using ultrasonic techniques. By using this method, the small local vibrations on various parts of a heart may ultimately be measured in a frequency range up to a few hundred Hertz. The thickness of the myocardium or the interventricular septum, which can be acoustically divided into two or three layers, is about 10 mm and the transition time of the ultrasonic wave is about 6 μs. Thus, in order to detect the

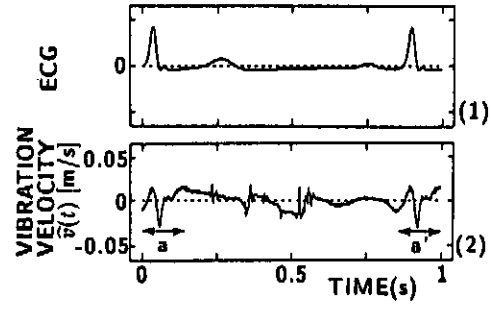

Fig. 7. Estimation results of small vibration on the wall of the interventricular septum in a young man. (1) The electrocardiogram (ECG). (2) The estimate of the vibration velocity on the wall of the interventricular septum.

vibration signal of each layer, it is necessary to transmit short length RF pulses and to use an A/D converted digital signal with a high frequency so that the pulses returning from the layers can be distinguished from each other with high spatial resolution.

By applying the signal processing described in [3] and [5] to the resultant vibration signals estimated by the method proposed in this paper, we may be able to diagnose the acoustic characteristics of various parts of the ventricle wall such as local plasticity and local elasticity, which depend on the dysfunction of the heart muscle.

Further investigation of this proposed method, including its clinical application, is being conducted.

Acknowledgment

The authors would like to thank Prof. Dr. Yoshiro Koiwa, Prof. Dr. Tamotsu, Takishima, and Prof. Dr. Kunio Shirado of Tohoku University, School of Medicine, Prof. Dr. Motonao Tanaka of the Institute of Development, Aging, and Cancer of Tohoku University, and Prof. Dr. F. Dunn of Bioacoustics Research Laboratory of University of Illinois for their suggestions. The authors are also grateful to Dr. T. Ono, Dr. H. Suzuki, and Dr. K. Yamaguchi of Ono Sokki Co. LTD., Mr. Y. Takeuchi of Yokogawa Medical Co. LTD., and Dr. Y. Honda of Honda Denshi Co. Ltd. for their support in the experiments. The authors also wish to acknowledge the assistance of Mr. D. Iwamoto, Mr. K. Kawabe, Mr. M. Takako, and Mr. R. Murata of our laboratory.

References

[1] Jules Constant, *Bedside Cardiology*. Boston, MA: Little Brown and Company, 1985.

[2] C. J. Hartley, H. Litowitz, R. S. Rabinovitz, W. X. Zhu, J. E. Chelley, L. H. Michael, and R. Bolli, "An ultrasonic method for measuring tissue displacement: Technical details and validation for measuring myocardial thickening," *IEEE Trans. Biomed. Eng.*, vol. 38, pp. 735–747, Aug. 1991.

[3] H. Kanai, N. Chubachi, K. Kido, Y. Koiwa, T. Takagi, J. Kikuchi, and T. Takishima, "A new approach to time-dependent AR modeling of signals and its application to analysis of the fourth heart sound," *IEEE Trans. Signal Processing*, vol. 40, pp. 1198–1205, May 1992.

[4] L. G. Durand, Y. E. Langlois, T. Lanthier, R. Chiarella, P. Coppens, S. Carioto, and S. Bertrand-Bradley, "Spectral analysis and acoustic transmission of mitral and aortic valve closure sounds in dogs. Part 1, modeling the heart/thorax acoustic system," *Med. Biological Eng. Comput.*, vol. 28, pp. 269–277, 1990.

[5] H. Kanai, Y. Shishido, N. Chubachi, Y. Koiwa, T. Takagi, J. Kikuchi, H. Honda, N. Hoshi, and T. Takishima, "Estimation of acoustic transfer function of the heart by analyzing the heart sounds simultaneously detected on the chest wall and in the esophagus," *Japanese J. Med. Electron. Biological Eng.*, vol. 6, no. 2, pp. 115–122, 1992 (in Japanese).
[6] S. Satomura, "Ultrasonic doppler method for the inspection of cardiac function," *J. Amer. Soc. Acoust.*, vol. 29, no. 11, pp. 1181–1185, Nov. 1957.
[7] D. W. Baker, "Pulsed ultrasonic doppler blood-flow sensing," *IEEE Trans. Sonic Ultrason.*, vol. SU-17, pp. 170–185, July 1970.
[8] F. D. McLeod and M. Anliker, "A multiple gate pulsed directional doppler flowmeter," in *Proc. IEEE Ultrason. Symp.*, Miami, FL, Dec. 1971.
[9] S. L. Johnson, D. W. Baker, R. A. Lute, and H. T. Dodge, "Doppler echocardiography," *Circulation*, vol. XLVIII, pp. 810–822, Oct. 1973.
[10] F. E. Barber, D. W. Baker, A. W. C. Nation, D. E. Strandness, Jr., and J. M. Reid, "Ultrasonic duplex echo-doppler scanner," *IEEE Trans. Biomed. Eng.*, vol. BME-21, pp. 109–113, Mar. 1974.
[11] C. J. Hartley, H. G. Hanley, R. M. Lewis, and J. S. Cole, "Synchronized pulsed doppler blood flow and ultrasonic dimension measurement in conscious dogs," *Ultrasound Med. Biology*, vol. 4, pp. 99–110, 1978.
[12] M. Brandestini, "Topoflow—A digital full range Doppler velocity meter," *IEEE Trans. Sonic Ultrason.*, vol. SU-25, pp. 287–293, Sept. 1978.
[13] E. Wildi, J. W. Knutti, H. V. Allen, and J. D. Meindl, "Dynamic and limitations of blood/muscle interface detection using doppler power returns," *IEEE Trans. Biomed. Eng.*, vol. BME-27, pp. 565–573, Oct. 1980.
[14] W. D. Barber, J. W. Eberhard, and S. G. Karr, "A new time domain technique for velocity measurements using doppler ultrasound," *IEEE Trans. Biomed. Eng.*, vol. BME-32, pp. 213–229, Mar. 1985.
[15] C. Kasai, K. Namekawa, A. Koyama, and R. Omoto, "Real-time two-dimensional blood flow imaging using an autocorrelation technique," *IEEE Trans. Sonic Ultrason.*, vol. SU-32, pp. 4587–463, May 1985.
[16] R. M. Olson and D. K. Shelton, "A nondestructive technique to measure wall displacement in the thoracic aorta," *J. Appl. Physiol.*, vol. 32, no. 1, pp. 147–151, Jan. 1972.
[17] R. M. Olson and J. P. Cooke, "A nondestructive ultrasonic technique to measure diameter and blood flow in arteries," *IEEE Trans. Biomed. Eng.*, vol. BME-21, pp. 168–171, 1974.
[18] J. O. Arndt, "The diameter of the intact carotid artery in man and its change with pulse pressure," *Pflüegers Archiv*, vol. 301, pp. 230–240, 1968.
[19] D. J. Mozersky, D. S. Sumner, D. E. Hokanson, and D. E. Strandness, Jr., "Transcutaneous measurement of the elastic properties of the human femoral artery," *Circulation*, vol. XLVI, pp. 948–955, Nov. 1972.
[20] A. P. G. Hoeks, C. J. Ruissen, P. Hick, and R. S. Reneman, "Transcutaneous detection of relative changes in artery diameter," *Ultrasound Med. Biology*, vol. 11, no. 1, pp. 51–59, 1985.
[21] W. T. Kemmerer, R. W. Ware, H. F. Stegall, J. L. Morgan, and R. Kirby, "Blood pressure measurement by doppler ultrasonic detection of arterial wall motion," *Surgery, Gynecology and Obstetrics*, vol. 131, pp. 1141–1147, Dec. 1970.
[22] K. Lindström, K. Marsal, G. Gennser, L. Bengtsson, M. Benthin, and P. Dahl, "Device for measurement of fetal breathing movements, I. The TD-recorder. A new system for recording the distance between two echogenerating structures as a function of time," *Ultrasound Med. Biol.*, vol. 3, pp. 143–151, 1977.
[23] I. Rupoport and A. J. Cousin, "New phase-lock tracking instrument for foetal breathing monitoring," *Med. Biologic. Eng. Comput.*, vol. 20, pp. 1–6, Jan. 1982.
[24] D. E. Hokanson, D. E. Strandness, Jr., and C. W. Miller, "An echo-tracking system for recording arterial wall motion," *IEEE Trans. Sonic Ultrason.*, vol. SU-17, pp. 130–132, July 1970.
[25] D. E. Hokanson, D. J. Monzersky, S. D. Sumner, and D. E. Strandness, Jr., "A phase-locked echo tracking system for recording arterial diameter changes *in vivo*," *J. Appl. Physiol.*, vol. 32, no. 5, pp. 728–733, May 1972.
[26] K. Nakayama and S. Sato, "Ultrasonic measurement of arterial wall movement utilizing phase-tracking system," in *Digest, 10th Int. Conf. Med. Biol. Eng.*, Dresden, 1973, p. 318.
[27] D. N. White and R. J. Stevenson, "Transient variations in the systolic pulsations in amplitude of intracranial echoes, their artificial origin," *Neurology*, vol. 26, pp. 683–689, 1976.
[28] C. F. Olsen, "Doppler ultrasound: A technique for obtaining arterial wall motion parameters," *IEEE Trans. Sonic Ultrason.*, vol. SU-24, pp. 354–358, June 1977.
[29] L. W. Korba, R. S. C. Cobbold, and A. J. Cousin, "An ultrasonic imaging and differential measurement system for the study of fetal respiratory movements," *Ultrasound Med. Biology*, vol. 5, pp. 139–149, 1979.
[30] D. H. Groves, T. Powalowski, and D. N. White, "A digital technique for tracking moving interfaces," *Ultrasound Med. Biology*, vol. 8, no. 2, pp. 185–190, 1982.
[31] L. S. Wilson and D. E. Robinson, "Ultrasonic measurement of small displacements and deformations of tissue," *Ultrason. Imaging*, vol. 4, pp. 71–82, 1982.

Hiroshi Kanai (A'89–M'91) was born in Matsumoto, Japan, on November 29, 1958. He received the B.E. degree from Tohoku University, Sendai, Japan in 1981, and the M.E. and the Dr. Eng. degrees, also from Tohoku University, in 1983 and in 1986, both in electrical engineering.

From 1986 to 1988 he was with the Education Center for Information Processing, Tohoku University, as a Research Associate. From 1990 to 1992 he was an Lecture at the Department of Electrical Engineering, Faculty of Engineering, Tohoku University. Since 1992 he has been an Associate Professor at the Department of Electrical Engineering, Faculty of Engineering, Tohoku University. His present interest is in digital signal processing and its application on the acoustical, ultrasonic, and electrical measurements.

Dr. Kanai is a member of the Acoustical Society of Japan, the Institute of Electronics Information and Communication Engineering of Japan, the Japan Society of Mechanical Engineers, the Japan Society of Ultrasonics in Medicine, Japan Society of Medical Electronics and Biological Engineering, the Institute of Electrical Engineers of Japan, and the Japanese Circulation Society.

Hiroaki Satoh was born in Miyagi, Japan, on July 7, 1966. He received the B.E. from Utsunomiya University, Japan, in 1989 in Electronic Engineering and M.E. degrees from Tohoku University, Sendai, Japan, in 1992 in Electrical and Communication Engineering. Since 1992 he has been a student in a doctor course of Electrical and Communication Engineering, Tohoku University, Japan. His current interest is in digital signal processing and ultrasonic measurements.

Mr. Satoh is a member of the Acoustical Society of Japan and the Japan Society of Ultrasonics in Medicine.

Kouichi Hirose was born in Tokyo, Japan, on March 10, 1969. He received the B.E. and M.E. degrees from Tohoku University, Sendai, Japan, in 1991 and in 1993, respectively, both in electrical engineering.

Since 1993 he has been with KDD, Japan.

Noriyoshi Chubachi (M'83) was born in Kokura, Japan, on October 5, 1933. He received the B.S., M.S., and Ph.D. degrees in electrical engineering from Tohoku University, Sendai, Japan, in 1956 and in 1962 and 1965, respectively.

In 1965, he joined the Research Institute of Electrical Communication, Tohoku University, where he was an Associate Professor from 1966 to 1978. Since 1979 he has been a Professor at the Department of Electrical Engineering, Tohoku University. From 1982 to 1983 he was a visiting Professor of Electrical and Computer Engineering, University of California, Santa Barbara, CA. He has worked on ultrasonic transducers and delay lines, surface acoustic devices, acoustoelectronics, piezoelectric materials, acoustic microscopy, and related problems.

Dr. Chubachi is a member of the Institute of Electronics and Communication Engineers of Japan, the Society of Japanese Applied Physics, the Acoustical Society of Japan, the Japan Society of Ultrasonics in Medicine, the Japan Society for Nondestructive Inspection, the Japan Society of Medical Electronics and Biological Engineering, the Japan Society of Mechanical Engineers, and the Institute of Electrical Engineers of Japan. He served as chairman, Tokyo chapter of IEEE UFFC Society, from 1987 to 1988.